Developmental Cognitive Neuroscience 39 (2019) 100682

Contents lists available at ScienceDirect

Developmental Cognitive Neuroscience

journal homepage: www.elsevier.com/locate/dcn

Structural and functional asymmetry of the language network emerge in early childhood

Jess E. Reynolds[a,b,c], Xiangyu Long[a,b,c], Melody N. Grohs[b,d,e], Deborah Dewey[b,c,f,g], Catherine Lebel[a,b,c,*]

[a] Department of Radiology, Canada
[b] Owerko Centre, Alberta Children Hospital Research Institute, Canada
[c] Hotchkiss Brain Institute, Canada
[d] Department of Neuroscience, Canada
[e] Cumming School of Medicine, Canada
[f] Department of Pediatrics, Canada
[g] Department of Community Health Sciences, Canada

ARTICLE INFO

Keywords:
Diffusion tensor imaging
Resting State fMRI
Asymmetry
Lateralization
Prereading
Arcuate Fasciculus

ABSTRACT

Structural and functional neuroimaging studies show language and reading processes are left-lateralized, and associated with a dispersed group of left brain regions. However, it is unclear when and how asymmetry of these regions emerges. We characterized the development of structural and functional asymmetry of the language network in 386 datasets from 117 healthy children (58 male) across early childhood (2–7.5 years). Structural asymmetry was investigated using diffusion tensor imaging (DTI) and manual delineation of the arcuate fasciculus. Functional connectivity asymmetry was calculated from seed regions in the inferior frontal gyrus (IFG) and middle temporal gyrus (MTG). We show that macrostructural asymmetry of the arcuate fasciculus is present by age 2 years, while leftward asymmetry of microstructure and functional connectivity with the IFG increases across the age range. This emerging microstructural and functional asymmetry likely underlie the development of language and reading skills during this time.

1. Introduction

Language and reading acquisition are dynamic processes that occur throughout childhood. Although reading development typically begins after a child reaches school age, the brain is primed for language while in utero (May et al., 2011), and pre-reading and language skills, such as phoneme identification and phonological awareness, start to develop during the first year of life (Dehaene-Lambertz et al., 2006a). Pre-reading skills and primary faculties of language (e.g., speaking and language comprehension) improve rapidly and fairly steadily across early childhood (2–7 years) (Lonigan et al., 2013; Torppa et al., 2006), and underlie the development of reading ability (Sakai, 2005). During early childhood, pre-reading language skills vary widely between children but tend to remain stable within individuals (Bornstein et al., 2004). Early language development lays the foundation for future reading skills, and measures such as phonological awareness and rapid naming are strong predictors of future reading success (Torppa et al., 2006).

Structural and functional neuroimaging studies have provided a better understanding of the neural correlates of language and reading (Sakai, 2005; Smits et al., 2014), and have shown that language and reading are left-lateralized (i.e., these processes are specialized to the left side of the brain), and associated with a dispersed group of left brain regions, including occipital-temporal, parietal-temporal, and inferior-frontal areas (Schlaggar and McCandliss, 2007), and the white matter tracts connecting them. The arcuate fasciculus is a key dorsal pathway within the language network (Hickok and Poeppel, 2004) that connects frontal (Broca's area) and temporo-parietal (Wernicke's area) language regions. It supports auditory-motor integration through the mapping of sound to motor representations, as well as phonological aspects of reading and speech (Saur et al., 2008; Vandermosten et al., 2012; Vigneau et al., 2006).

The findings across studies are inconsistent regarding the age at which structural asymmetry (i.e., differences between hemispheres) of the arcuate emerges. Some studies report leftward microstructural (fractional anisotropy measured by diffusion imaging, myelin water

* Corresponding Author at: Room B4-513, Alberta Children's Hospital, 28 Oki Drive NW, Calgary, Alberta, T3B 6A8, Canada.
E-mail address: clebel@ucalgary.ca (C. Lebel).

https://doi.org/10.1016/j.dcn.2019.100682
Received 21 March 2019; Received in revised form 18 June 2019; Accepted 17 July 2019
Available online 21 July 2019

fraction) (Dubois et al., 2008; O'Muircheartaigh et al., 2013) or macrostructural (fiber connection locations) (Perani et al., 2011) asymmetry in infants. Others report a relatively symmetrical pattern of micro- (Salvan et al., 2017; Song et al., 2014) and macrostructure (volume) (Song et al., 2014), with microstructural asymmetry evident after age 9 years (Tak et al., 2016). Stable leftward asymmetry of the arcuate macrostructure (number of streamlines) has been demonstrated in adults, and children as young as 5 years (Lebel and Beaulieu, 2009; Qiu et al., 2011), but it is unclear when this emerges. Furthermore, studies have reported mixed findings regarding whether asymmetry confers an advantage for language or reading skills. Increased leftward asymmetry of the arcuate has been associated with better phonological skills (Lebel and Beaulieu, 2009) and reading scores in children as young as 5 years (Qiu et al., 2011); however, other research has found that a more symmetrical arrangement of the arcuate fasciculus is related to better receptive language and reading skills in children and adults (Catani et al., 2007; Yeatman et al., 2011). Asymmetry is often considered beneficial; however, it is unclear whether potential benefits vary across different developmental stages. Therefore, to gain a better understanding asymmetry and how it may relate to pre-reading measures, it is important to investigate structural and functional asymmetry of brain regions before children are able to read.

Leftward asymmetry of functional language networks has been identified in neonates (Pena et al., 2003) and young children (Dehaene-Lambertz et al., 2002, 2006b), with asymmetry increasing from late childhood into early adulthood (Perani et al., 2011; Szaflarski et al., 2006). In school-aged children, it has been suggested that the extent and locations of left lateralization are task dependent, and that age-related increases in lateralization may be tied to the developmental timing of language skill development (Holland et al., 2007). Little research has been undertaken during early childhood, but one cross sectional resting state fMRI study demonstrated a more leftward asymmetrical language network in 5-year-old children compared to 3-year-old children (Xiao et al., 2016a). It is unclear how functional asymmetry relates to language abilities; however, a longitudinal study of 5-year old children enrolled in kindergarten showed increasing leftward lateralized functional activation for a letter task over 3 months (Yamada et al., 2011).

Significant brain development occurs in early childhood, which is also a critical time for the development of language and reading skills. However, it is unclear whether structural or functional asymmetry of reading areas is present in young children, and how these are associated with emerging language abilities. A more comprehensive understanding of typical brain structural and functional development across this pre-reading period in reading related areas, and the relationship with pre-reading and later reading development, is important for future research investigating the associations between brain structure and function, and reading disorders in children. While reading disorders are typically not identified until school age, research suggests that differences in brain structure precede reading difficulties (Raschle et al., 2011; Walton et al., 2018). Understanding the links between brain asymmetry development and the emergence of reading skills, may ultimately help identify early brain biomarkers that could be used to identify children who will go on to develop reading difficulties. This could facilitate earlier diagnosis, help identify key regions to target for early intervention approaches, and allow for monitoring of brain changes during interventions. The aim of this study was to determine the developmental trajectories of structural (arcuate fasciculus) and functional (intra - and inter-hemispheric functional connectivity from the inferior frontal gyrus (IFG) and the middle temporal gyrus (MTG)) asymmetry of key language regions, and their relationship with pre-reading skills, across early childhood (2–7.5 years) using DTI and passive viewing fMRI. Furthermore, we aimed to explore what was driving any changes in asymmetry (e.g., faster development of left hemisphere structures, left development/right stability). We hypothesised that pre-reading measures would be related to brain structure and function across this early childhood period.

Although some studies use the terms asymmetry and lateralization interchangeably, here we use asymmetry to refer to differences in structure or function between brain hemispheres, and lateralization to refer to the specialization of processes to one side of the brain.

2. Methods

2.1. Subjects

One-hundred and seventeen children (58 male; 95RH/11LH/11 undecided handedness – parent report) aged 1.95–6.97 years at intake (mean = 3.97 ± 1.02 years; longitudinal age range = 1.95–7.625 years) were recruited from the local community and an ongoing prospective study (Kaplan et al., 2014) to undergo MRI. Children returned for follow-up scans (average time between visits = 7.8 ± 4.6 months based on diffusion scans). One-hundred and sixteen children had between 1–20 diffusion MRI scans each (one scan: 39 children; two scans: 22; three scans: 8; four scans: 11; five scans: 14; six scans: 12; seven scans: 8; 12 scans: 1; and twenty scans: 1). Sixty-seven of these children, and one additional child (68 children, 173 datasets) participated in a passive viewing task-free fMRI (resting state) scan (one scan: 23 children; two scans: 14; three scans: 14; four scans: 8; five scans: 6; six scans: 3). Not all children had usable fMRI data due to time restrictions (fMRI was later in the protocol), motion artifacts, or because they were asleep. A summary of participant data is presented in Table 1. All children were free from diagnosed neurological disorders and were born ≥35 weeks' gestation. Parental/guardian written informed consent, and child assent were obtained for each participant. The University of Calgary Conjoint Health Research Ethics Board (CHREB) approved this study (REB13-0020).

Table 1
Summary of participant data for MRI scans and pre-reading assessments. Age is in years.

	DTI	rsfMRI	Phonological Processing	Speeded Naming	Right Arcuate
DTI					
n_{scans} ($n_{participants}$)	381 (116)	168 (67)	331 (108)	324 (107)	343 (106)
Mean age (range)	4.61 (1.95-7.625)	4.61 (1.97-6.97)	4.79 (3.00-7.625)	4.77 (3.00-7.625)	4.60 (1.95-7.61)
rsfMRI					
n_{scans} ($n_{participants}$)		173 (68)	160 (66)	157 (66)	
Mean age (range)		4.60 (1.97-6.97)	4.70 (3.00-6.97)	4.71 (3.00-6.97)	
Phonological Processing					
n_{scans} ($n_{participants}$)			336 (110)	329 (108)	295 (99)
Mean age (range)			4.78 (3.00-7.625)	4.76 (3.00-7.625)	4.80 (3.00-7.61)
Speeded Naming					
n_{scans} ($n_{participants}$)				329 (108)	288 (98)
Mean age (range)				4.76 (3.00-7.625)	4.78 (3.00-7.61)

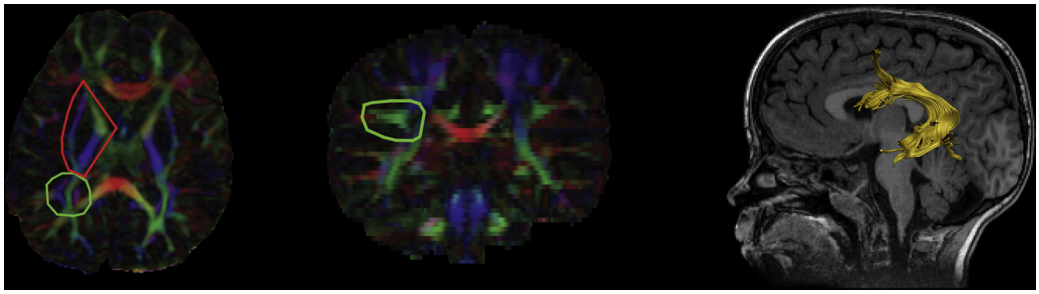

Fig. 1. Left arcuate fasciculus manual tractography inclusion/seed (green), and exclusion (red) regions of interest, and left arcuate fasciculus.

2.2. Language assessments

Children over 3 years (3.003–7.625 years; NEPSY-II age band starts at 3 years) had their pre-reading abilities assessed using the NEPSY-II Phonological Processing and Speeded Naming subtests on the same day as scanning, or as part of a comprehensive neuropsychological assessment (approx. 20 min.; Table 1). The Phonological Processing subtest assesses phonemic awareness and the Speeded Naming subtest assesses rapid semantic access to, and production of, names of colors and shapes (Korkman et al., 2007). Because the assessments are slightly different for different age bands and Speeded Naming is broken into two components (number correct and time), age standardized scores were calculated for the Phonological Processing and Speeded Naming subtests (Korkman et al., 2007). Throughout early childhood pre-reading skills tend to remain stable within individuals (Bornstein et al., 2004), and these measures have been found to be good predictors of later reading abilities (Logan et al., 2011).

Table 1 provides information on the number of children with pre-reading measures. Standardized Phonological Processing scores (n = 336) ranged from 3 to 19 (mean ± SD = 11.5 ± 2.7); Standardized Speeded Naming scores (n = 329) ranged from 3 to 19 (mean ± SD = 12.0 ± 2.7). These means are slightly higher than the standardized population norm of 10 ± 3.

2.3. MRI image acquisition

All imaging was conducted using the same General Electric 3 T MR750w system and a 32-channel head coil (GE, Waukesha, WI) at the Alberta Children's Hospital in Calgary, Canada. Children were scanned either while awake and watching a movie of their choice, or while sleeping without sedation. fMRI scans during which the child was asleep were excluded from analyses. Prior to scanning, parents were provided with detailed information on MRI procedures and were given the option to complete a practice MRI session in a training scanner to familiarize the child with the scanning environment, or to make use of a take home pack with information about MRI scans (e.g., noise recordings (Thieba et al., 2018)).

Whole-brain diffusion weighted images were acquired using single shot spin echo echo-planar imaging sequence: 1.6 × 1.6 × 2.2 mm resolution (resampled on scanner to 0.78 × 0.78 × 2.2 mm), full brain coverage, TR = 6750 ms; TE = 79 ms (set to minimum for first year), 30 diffusion encoding gradient directions at b = 750 s/mm^2, and five interleaved images without diffusion encoding at b = 0 s/mm^2 for a total acquisition time of approximately four minutes.

T1-weighted images were acquired using a FSPGR BRAVO sequence, 210 axial slices; 0.9 × 0.9 × 0.9 mm resolution, TR = 8.23 ms, TE = 3.76 ms, flip angle = 12°, matrix size = 512 × 512, inversion time = 540 ms.

Passive viewing fMRI data were acquired with a gradient-echo echo-planar imaging (EPI) sequence, 36 axial slices, 3.59 × 3.59 × 3.6 mm resolution, TR = 2000 ms, TE = 30 ms, flip angle = 60°, matrix size = 64 × 64, 250 volumes.

2.4. Data processing

DTI data was visually quality checked to remove motion-corrupted volumes and volumes with artifacts (e.g. venetian blinds, mechanical vibration). Entire datasets were excluded if more than 12 diffusion weighted volumes were removed. Of the participants included in the analyses reported here (116 participants, 381 scans), the average number of volumes remaining was 27.4 ± 3.0 (range = 18–30) diffusion weighted and 4.8 ± 0.5 (range = 2–5) b0 images. Following corrupted volume removal, data was pipelined through ExploreDTI V4.8.6 (Leemans et al., 2009) for the remainder of preprocessing. Correction for signal drift, Gibbs ringing (non-DWIs), subject motion, and eddy current distortions were performed (Leemans and Jones, 2009).

Fiber tracking was performed using a deterministic streamline method in ExploreDTI. A minimum FA threshold was set to 0.20 to initiate and continue tracking, and angle threshold set to 30°. While semi-automated tractography methods are well suited to delineate a range of fiber tracts, this method is not as appropriate to isolate fronto-temporal arcuate fibers from superior longitudinal fasciculus fibers (Lebel and Beaulieu, 2009), so tracts were isolated manually. Using a priori information on arcuate fasciculus tract location (Lebel and Beaulieu, 2009; Wakana et al., 2004), seed, inclusion, and exclusion regions of interest (ROIs) were drawn on the left and right hemisphere separately, in each subject (Fig. 1). One inclusion/seed region was defined on a coronal slice where the arcuate fasciculus (appearing as a green – anterior-posterior fiber direction – triangle) was visibly the largest. A second inclusion ROI was drawn on the axial slice where the arcuate passes in an inferior-superior direction (dark blue). Both inclusion ROIs were drawn large enough (approx. 5 mm margin around tract) to ensure that all arcuate fibers were included in the tract. An exclusion region was drawn over the internal and external capsules. All tracts were quality checked and further small manual edits (exclusion ROIs) were drawn as required to remove spurious fibers. The operator was blind to participant ID, age, and the pre-reading measures. The number of streamlines, and mean values of FA, and MD (mm^2/s) were extracted for each tract. Tracts with fewer than 10 streamlines were deemed unsuccessful and excluded from analysis. The left arcuate was successfully delineated in all datasets. The right arcuate was successfully delineated in 343 datasets (90%).

For the fMRI data preprocessing, the first 10 time points were removed for the purpose of MR signal stabilization. Pre-processing included correction of slice timing and head motion, co-registration to the T1 image (manually quality checked for motion or artifacts), and linear de-trending of signals. The relative root-mean-square frame-wise displacement (FD) was calculated (Jenkinson et al., 2002). A multi-parameter regression model included signals from the non-grey matter regions, head motion and spikes (relative FD > 0.25 mm) were regressed out of the pre-processed fMRI data (Long et al., 2017). Participants with high mean relative FD (> 0.25 mm) or signals shorter than 4 min after removal of the spike time points were excluded (Satterthwaite et al., 2013). Finally, the processed fMRI signals were band-pass filtered

(0.009 to 0.08 Hz) and spatially normalized to 3 × 3 × 3 mm using a symmetrical pediatric template, which was created by averaging a pediatric brain template (ages 4.5–8.5 years) in Montreal Neurological Institute (MNI) standard space (Fonov et al., 2011) and its left-right flipped version. All steps were done using AFNI (version AFNI_16.2.12) (Cox, 1996) and FSL (Jenkinson et al., 2012).

Two seed regions that are key components of the language network (Xiao et al., 2016a; Houdé et al., 2010) were selected to investigate left and right hemisphere functional connectivity patterns, as well as intra- and inter-hemispheric functional asymmetry. Two ROI spheres (radius = 6 mm) were centered over the inferior frontal gyrus (IFG; pars triangularis, Broca's area, x = −49, y = 31, z = 6) and the middle temporal gyrus (MTG; close proximity to Wernicke's area, x = −52, y = −41, z = 6), based on pre-defined coordinates from a fMRI meta-analysis of reading in children (Houdé et al., 2010). Seed ROIs were defined in the left hemisphere, and then left-right flipped to create a symmetrical ROI in the right hemisphere. Functional connectivity maps of those seed regions were created and converted to *z*-maps by Fisher's transformation. A symmetric grey matter mask (46,242 voxels) was created from the symmetric pediatric T1 image template and applied to all functional connectivity z-maps for the further analysis.

To determine functional asymmetry of the language network, the *z*-maps calculated from the seeds in the right hemisphere were left-right flipped, and an asymmetry index map was created for each participant by subtracting the right flipped map from the left hemisphere seeded map (Asymmetry Index $[AI_{Functional}] = z\text{-}FC_{Left\ ROI} - z\text{-}FC_{Right\ ROI\ Flipped}$). From the resultant $AI_{Functional}$ map, results in the left hemisphere reflect asymmetry in intrahemispheric functional connectivity (left to left hemisphere FC – measured in the left z-map compared to right to right hemisphere FC – measured in the right flipped map), and results in the right hemisphere reflect interhemispheric asymmetry (left to right hemisphere FC compared to right to left hemisphere FC). In both cases, higher values indicate more connectivity from left hemisphere seeds.

2.5. Statistical analysis

Statistics for DTI parameters and extracted fMRI parameters were performed using RStudio version 1.1.453 (RStudio Team, 2016), and the 'lme4' (Bates et al., 2015), and 'lmerTest' (Kuznetsova et al., 2017) packages. SPSS (Version 24.0.0.1; IBM Corp, 2016) was used to examine changes in pre-reading scores with age. To examine asymmetry of the arcuate fasciculus, an asymmetry index (AI = [Left-Right]/[Left + Right]) was calculated for the number of streamlines (AI > 0 = leftward asymmetry; AI < 0 = rightward asymmetry), FA (AI > 0 = higher left FA; AI < 0 = higher right FA), and MD (AI < 0 = lower left MD; AI > 0 = lower right MD), where AI was a continuum from −1 to 1. For scans where only the left arcuate could be delineated, $AI_{streamlines}$ was 1 (left – zero/left + zero = 1). These scans were excluded from FA and MD asymmetry calculations. While scans with $AI_{streamlines} = 1$ were included, sub-analyses for $AI_{streamlines}$ were also run excluding the scans of these datasets. FA and MD asymmetry indices were scaled ($x10^2$), to bring them to a closer scale to other measures.

Linear mixed effects models were run to determine the development trajectories of the AIs ($AI_{Streamlines}$: asymmetry of number of streamlines; AI_{FA}: fractional anisotropy asymmetry; AI_{MD}: mean diffusivity asymmetry), as well as the left and right arcuate fasciculus (FA, MD) across the age range. Age, sex, and handedness were modelled as fixed predictors and subject modelled as a random factor (AI or Left/Right Arcuate microstructure = age + sex + handedness + (1|Subject)). MD values were scaled ($x10^3$) for analyses to bring them to a similar scale as age and pre-reading measures.

Changes in asymmetry of functional connectivity with age were similarly examined controlling for sex and handedness. To determine the development of asymmetry of connectivity with these seeds with age, a binary 173 × 50 matrix including a constant column, sex, handedness, mean FD, and longitudinal information was created, and regressed out of age and the $AI_{Functional}$ maps. In each column of the matrix, multiple scans for the same individual were indicated with a 1 and all other scans were set to 0, allowing the shared variance across multiple scans to be statistically accounted for. Linear (Pearson) correlations were run to test the relationships between the $AI_{Functional}$ maps and age using the robust correlation toolbox (Pernet et al., 2013). For each voxel within the symmetric GM mask, the robust correlation paradigm was performed between each $AI_{Functional}$ value and age across all datasets. Results were determined to be statistically significant (voxel-wise $p < 0.01$) based on the confidence interval from the bootstrapping analysis. Finally, the correlation map was corrected for multiple comparisons to $p < 0.05$ (voxel-wise $p < 0.01$, cluster size of age data > 12,123 mm^3) by 3dClustSim with the averaged estimated smoothing parameters by 3dFWHMx in AFNI (version: AFNI_16.2.12 (Cox, 1996)). Therefore, the final clusters reported survived both the permutation test during correlation and the cluster-level correction. Connectivity and asymmetry results are displayed using BrainNet Viewer (Xia et al., 2013).

For follow-up analyses to extract the AI values and the left/right z-map components from the regions showing significant changes in AI with age (see below), 6 mm ROIs were created, centered over the peak voxels from the $AI_{Functional}$ correlation maps (x = −25, y = 31, z = −15; x = 32, y = 7, z = 12). Using these ROIs, average $AI_{Functional}$ values were extracted from each individuals' $AI_{Functional}$ maps, and the left and right flipped *z* maps (from the corresponding seed).

2.6. Development of pre-reading skills across the preschool period

To assess whether pre-reading scores remained stable within individuals relative to their peers, slopes were calculated for pre-reading measures in participants with two or more pre-reading standard scores, using all time points where pre-reading assessments were completed. Linear regression was used to predict pre-reading values within subjects. Slope was then calculated as change in predicted standard score, divided by the change in age in years. One sample t-tests were run to assess change for individuals with two or more assessments, and for individuals with three or more assessments, with a test value of 0.

2.7. Relationships between structure, function, asymmetry, and pre-reading skills

Linear mixed effects models were run to determine the relationship between age-standardized Phonological Processing and Speeded Naming scores, and asymmetry indices for both structural and functional connectivity: Pre-reading = AI + Sex + Handedness + (1|Subject). For functional connectivity, the extracted $AI_{Functional}$ values for each significant region were used.

To further examine relationships between asymmetry and pre-reading ability, as well as to enable comparison with previous studies, we also investigated the associations between FA and MD in the left and right arcuate fasciculi and pre-reading measures (Pre-reading = Microstructure + Sex + Handedness + (1|Subject)). Furthermore, we tested relationships between extracted connectivity values from the left and right seeds, and pre-reading scores using linear mixed models as above.

2.8. Data availability

Neuroimaging data used in this study are freely available on the Open Science Framework: http://

doi.org/10.17605/OSF.IO/AXZ5R. Code used in this study will be made available upon request to the corresponding and/or first author.

Table 2
Linear mixed effects model parameter estimates for arcuate fasciculus macrostructural (streamlines) and microstructural (FA, MD) asymmetry indices. AI_{MD} and AI_{FA} values were scaled by 10^2 for analyses. Significance levels presented as *** < 0.001, ** < 0.01, * < 0.05.

	Intercept	Age (years)	Sex (male)	Handedness	
				Left	Undecided
$AI_{Streamlines}$	0.349 ± 0.072***	0.009 ± 0.011	−0.012 ± 0.067	−0.056 ± 0.113	0.103 ± 0.127
AI_{MD}	1.334 ± 0.335***	−0.174 ± 0.058**	−0.258 ± 0.261	−0.199 ± 0.414	0.685 ± 0.548
AI_{FA}	0.342 ± 0.707	0.102 ± 0.114	0.583 ± 0.607	0.456 ± 0.974	0.111 ± 1.237

3. Results

3.1. Structural asymmetry

Leftward asymmetry for number of streamlines ($AI_{Streamlines} > 0$) was noted in 83.7% of scans (mean $AI_{Streamlines} = 0.42 \pm 0.38$) and was not significantly associated with age ($p = 0.390$; Table 2). Additional analyses for $AI_{Streamlines}$ were run, excluding those where only the left arcuate could be delineated (e.g., excluding those with $AI_{Streamlines} = 1$; Yeatman et al., 2011), and results (e.g., age and pre-reading) were unchanged. Most children (64.1% of scans) had leftward asymmetry for FA ($AI_{FA} > 0$; mean $AI_{FA} = 0.015 \pm 0.035$); this asymmetry was not significantly associated with age ($p = 0.370$) (Fig. 2 and Table 2). There was leftward asymmetry for MD ($AI_{MD} < 0$; lower MD in left hemisphere) in 44.9% of scans (mean $LI_{MD} = 0.003 \pm 015$). AI_{MD} was negatively associated with age ($p = 0.003$), indicating a reduction of rightward asymmetry, and a shift towards leftward asymmetry across early childhood (Table 2).

FA increased with age at similar rates in the left and right arcuate fasciculi (Fig. 2B inset). MD decreased with age in both the left and right arcuate fasciculi, but the slope was steeper in the left, thus driving the reduced rightward MD asymmetry that was seen with age (Fig. 3C inset).

3.2. Development of functional asymmetry

Fig. 3 shows the relationships between asymmetry of functional connectivity from the IFG seed region and age. Intra-hemispheric (results from left hemisphere AI map) leftward asymmetry of connectivity between the IFG seed and neighbouring regions of the IFG, the premotor area, insula, putamen and anterior superior temporal gyrus increased with age. Inter-hemispheric (results from right hemisphere AI map) leftward asymmetry of connectivity between the pars triangularis seed and the orbitofrontal cortex, anterior prefrontal cortex, pars opercularis, pars orbitalis, insula and the anterior superior temporal gyrus increased with age. At the group level, these changes represent an increase in left hemisphere connectivity, and a decrease or no change of right hemisphere connectivity. This is reflected by a shift from slightly rightward asymmetry or symmetrical patterns of asymmetry in younger children (i.e., 2–3 years of age), to leftward asymmetry in older children. No clusters from the MTG survived multiple comparisons corrections (cluster corrected to $p < 0.05$).

3.3. Pre-reading development across the preschool period

In this dataset, the average slope (± SD) for individuals with two or more pre-reading measures ($n = 75$) on the Phonological Processing standard score was 0.69 ± 2.64 points per year (95% CI = 0.08–1.30, t = 2.265, $p = 0.026$), and for those with three or more datasets ($n = 50$), it was 0.70 ± 1.79 points per year (95% CI = 0.19–1.21, t = 2.76, $p = 0.008$). The average slope (± SD) for individuals with more two or more pre-reading measures ($n = 74$) on the Speeded naming standard score was 0.64 ± 3.24 standard points per year (95% CI = −0.11–1.39, t = 1.69, $p = 0.095$), and for those with three or more datasets ($n = 50$), it was 0.21 ± 1.73 (95% CI = −0.28–0.70, t = 0.85, $p = 0.400$).

3.4. Relationships between arcuate fasciculus, structural and functional asymmetry, and pre-reading skills

Phonological Processing scores were not significantly related to asymmetry of streamlines ($p = 0.495$), FA ($p = 0.409$), or MD ($p = 0.320$) (Table 3). Similarly, Speeded Naming scores were not related to asymmetry of streamlines ($p = 0.152$), FA ($p = 0.405$), or MD ($p = 0.123$) (Table 4).

In the left arcuate, FA was positively related to Phonological

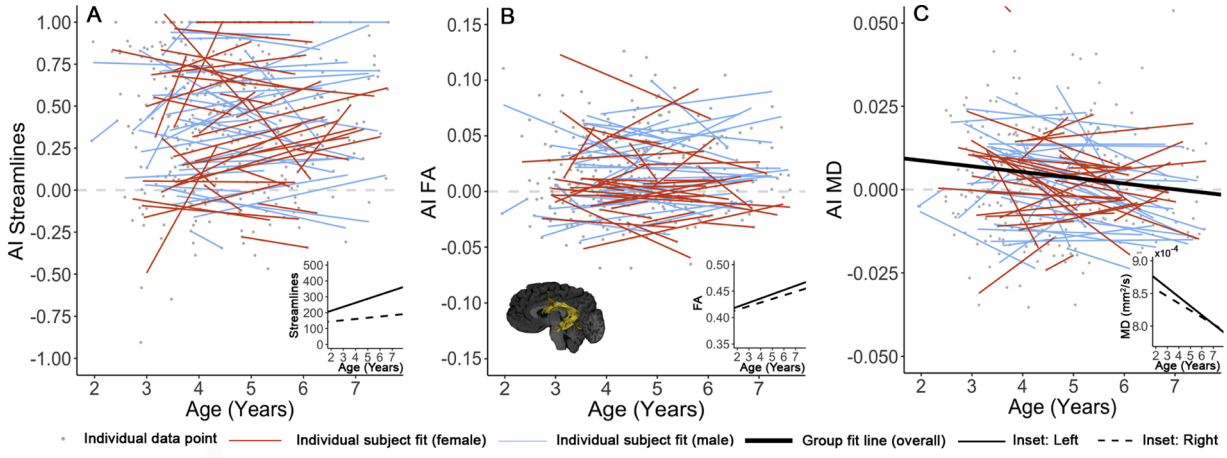

Fig. 2. Relationship between arcuate fasciculus asymmetry indices (AI) and age (A: number of streamlines; B: fractional anisotropy (FA); and C: mean diffusivity (MD)). For streamlines and FA, asymmetry indices > 0 (above dashed line) indicate leftward asymmetry, and for MD asymmetry indices < 0 indicate leftward asymmetry. Linear best fit lines for each individual subject are shown with orange red (girls) and pale blue lines (boys). Individual data points are shown in grey. Left (solid black line) and right (dashed black line) components of asymmetry indices are shown as insets in each asymmetry plot.

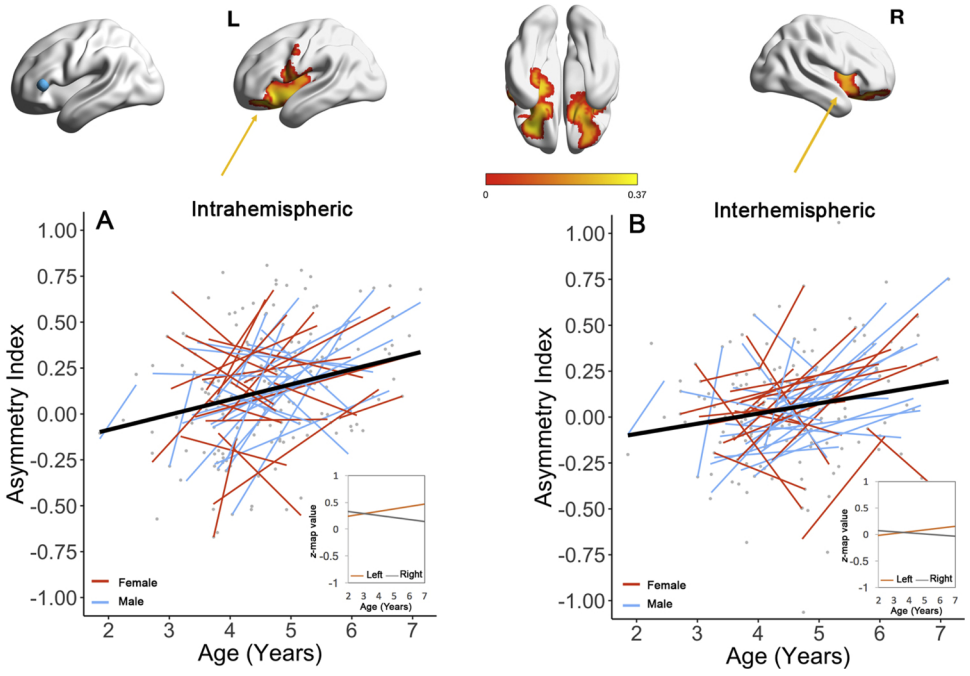

Fig. 3. Brain figures show leftward asymmetry of intra- and inter-hemispheric connectivity between the inferior frontal gyrus (IFG) pars triangularis seed (shown in blue), and the IFG, premotor area, insula, putamen and anterior superior temporal gyrus increased with age (sex, handedness, and mean FD are regressed out of age and functional AI and component values). Results shown in the left hemisphere reflect changes in intrahemispheric connectivity, and results in the right hemisphere reflect changes in interhemispheric connectivity. Positive correlations with seed regions and age are shown in red to yellow. 3A and 3B: Asymmetry indices (AIs; grey dots) were extracted from regions of interest centered on peak coordinates indicated by the arrows (3A. left/intrahemispheric: x = −25, y = 31, z = −15; 3B. right/interhemispheric: x = 32, y = 7, z = 12) and are plotted against age. Best fit lines for the entire dataset are shown in black. Best fit lines for each individual subject are shown with thinner red (girls) and blue lines (boys). Insets of the left (orange line) and right (grey line) z-map components of the AI of these peak regions are shown.

Processing ($p = 0.004$), but not Speeded Naming ($p = 0.164$). Left MD was negatively related to Speeded Naming ($p = 0.027$) and Phonological Processing ($p = 0.023$) (Table 3 and Table 4; Supplementary Fig. 1). No significant relationships between the right arcuate and pre-reading measures were identified ($p > 0.05$).

No significant relationships between functional connectivity asymmetry and Phonological Processing or Speeded Naming were identified (all $p > 0.05$).

4. Discussion

We showed that leftward asymmetry of the arcuate fasciculus macrostructure (i.e., number of streamlines) is established by 2 years of age, but microstructural and functional leftward asymmetry develops across early childhood. Unlike previous findings in older children and adults, asymmetry was not related to pre-reading language abilities, suggesting that this relationship may not emerge until children begin reading. Some slight changes were seen in terms of how individual's pre-reading skills compared to population norms across the time. The high standard deviations and wide 95% confidence intervals, suggest that while as a group, pre-reading skills remained relatively consistent across the preschool period (e.g., Bornstein et al., 2004) with only slight (< 1 standard point per year) increases in phonological processing standard scores, there is some variability in scores and skill development relative to peers at an individual level.

The majority of children had leftward asymmetry of arcuate fasciculus macrostructure, with a higher number of streamlines in the left compared to the right hemisphere, consistent with previous research in older children (Lebel and Beaulieu, 2009; Qiu et al., 2011; Yeatman et al., 2011). This asymmetry remained stable across the 2–7.5 year age range. Given that previous studies have also found no significant changes in macrostructural asymmetry of the arcuate with age (Lebel and Beaulieu, 2009; Qiu et al., 2011), our findings suggest that the macrostructural asymmetry of the arcuate is fully established by 2 years of age, well before reading begins. Considerable heterogeneity was observed in asymmetry between individuals, with approximately 15% of the scans showing some degree of right asymmetry for streamlines. Heterogeneity was present across the age range, however, individuals had relatively stable asymmetry values across period; individuals above the mean stayed above, and individuals below the mean and those showing rightward patterns stayed below. This suggests the heterogeneity in the dataset reflects individual variation rather than measurement error. Furthermore, patterns of asymmetry were not influenced by handedness. This is similar to previous studies noting that between 4–17% of participants have some degree of rightward asymmetry (Lebel and Beaulieu, 2009; Catani et al., 2007; Qiu et al., 2011; Yeatman et al., 2011).

In contrast to the established macrostructural asymmetry, decreasing rightward, and emerging leftward asymmetry of arcuate microstructure and functional connectivity of language regions was

Table 3
Linear mixed effects model parameter estimates for relationship between pre-reading (Phonological Processing) and arcuate fasciculus macrostructural (streamlines) and microstructural (FA, MD) asymmetry indices, and left and right arcuate fasciculus microstructure (FA, MD). AI_{MD} and AI_{FA} values were scaled by 10^2, and MD values were scaled by 10^3 for analyses. Significance levels presented as *** < 0.001, ** < 0.01, * < 0.05.

Phonological Processing	Intercept	AI/Microstructure Measure	Sex	Handedness	
				Left	Undecided
$AI_{Streamlines}$	11.187 ± 0.357***	0.318 ± 0.465	0.009 ± 0.399	0.226 ± 0.637	−1.177 ± 1.025
AI_{MD}	11.241 ± 0.326***	−0.107 ± 0.108	0.146 ± 0.428	0.220 ± 0.655	−0.714 ± 1.107
AI_{FA}	11.160 ± 0.327***	0.043 ± 0.052	0.135 ± 0.431	0.217 ± 0.658	−0.884 ± 1.098
Left FA	0.445 ± 3.738	24.417 ± 8.369**	0.062 ± 0.398	0.490 ± 0.642	−1.094 ± 1.016
Left MD (mm^2/s)	21.984 ± 4.670***	−12.958 ± 5.662*	0.208 ± 0.406	0.349 ± 0.635	−0.804 ± 1.028
Right FA	7.340 ± 2.670**	8.731 ± 6.013	0.254 ± 0.439	0.385 ± 0.675	−0.812 ± 1.103
Right MD (mm^2/s)	18.927 ± 4.846***	−9.481 ± 5.924	0.340 ± 0.447	0.373 ± 0.670	−0.898 ± 1.101

Table 4
Linear mixed effects model parameter estimates for relationship between pre-reading (Speeded Naming) and arcuate fasciculus macrostructural (streamlines) and microstructural (FA, MD) asymmetry indices, and left and right arcuate fasciculus microstructure (FA, MD). AI_{MD} and AI_{FA} values were scaled by 10^2, and MD values were scaled by 10^3 for analyses. Significance levels presented as *** < 0.001, ** < 0.01, * < 0.05.

Speeded Naming	Intercept	AI/Microstructure Measure	Sex	Handedness	
				Left	Undecided
$AI_{Streamlines}$	11.772 ± 0.344***	0.649 ± 0.452	−0.259 ± 0.385	0.061 ± 0.611	−2.415 ± 0.991*
AI_{MD}	12.105 ± 0.318***	−0.169 ± 0.109	−0.388 ± 0.417	0.028 ± 0.633	−2.114 ± 1.094
AI_{FA}	12.006 ± 0.317***	0.043 ± 0.051	−0.390 ± 0.417	0.027 ± 0.631	−2.394 ± 1.082*
Left FA	6.901 ± 3.686	11.531 ± 8.258	−0.231 ± 0.392	0.143 ± 0.630	−2.331 ± 0.998*
Left MD (mm^2/s)	22.395 ± 4.664***	−12.594 ± 5.656*	−0.064 ± 0.398	0.168 ± 0.621	−2.012 ± 1.004*
Right FA	11.670 ± 2.636***	0.840 ± 5.945	−0.351 ± 0.423	0.061 ± 0.644	−2.372 ± 1.087*
Right MD (mm^2/s)	15.756 ± 4.890**	−4.552 ± 5.976	−0.279 ± 0.431	0.1137 ± 0.641	−2.398 ± 1.085*

observed across early childhood. For both structure and function, the decreases in rightward asymmetry (AI_{MD}) and increasing leftward asymmetry ($AI_{Functional}$) was driven by more rapid changes in the left hemisphere. MD decreases are consistent with known developmental patterns (Reynolds et al., 2019), and here suggest greater maturation within the left arcuate. Changes in arcuate FA and MD likely reflect increasing myelination and/or axonal packing (Lebel et al., 2017). No previous studies have examined age-related changes in the asymmetry of arcuate microstructure in young children longitudinally, but some reports suggest that left arcuate microstructural properties (i.e., FA and MD) mature faster than the right in later childhood and adolescence (Eluvathingal et al., 2007), suggesting increasing leftward asymmetry with age.

Age-related increases of leftward asymmetry were also evident for intra- and inter-hemispheric functional connectivity. In general, left hemisphere language regions seeds became more functionally connected across the age range, while connectivity from right hemisphere seeds decreased slightly or did not change. These results are broadly consistent with the patterns of development observed in cross sectional research by Xiao et al. (2016a), who found increased leftward asymmetry of connectivity from the IFG and posterior superior temporal gyrus in 5-year olds compared to 3-year olds. Older children have been found to show leftward lateralization that continues to increase into adolescence (Holland et al., 2007), suggesting that ongoing functional specialization commences in early childhood and continues through adolescence. The increasing leftward asymmetry of intra-hemispheric connectivity between the IFG and anterior superior temporal gyrus seen in the present study may reflect development of the ventral language pathway, which supports sound to meaning integration processes (Saur et al., 2008). Given that the ventral pathway supports higher-level language comprehension (Saur et al., 2008), which is still developing across this period of early childhood, this may be an important period in the development of lateralization of these processes in the brain. These increases in intra-hemispheric left asymmetry may also represent a strengthening of intra-hemispheric connectivity and a shift from more inter- to intra-hemispheric connectivity patterns with age (Friederici et al., 2011; Perani et al., 2011; Yamada et al., 2011; Youssofzadeh et al., 2018) as language networks are refined.

Interestingly, none of changes in macrostructural, microstructural, or functional asymmetry with age were related to pre-reading language skills in young children. Previous research in school-aged children has observed relationships between reading/language ability and structural asymmetry, generally finding that leftward asymmetry of the arcuate fasciculus is related to better reading scores (Lebel and Beaulieu, 2009; Qiu et al., 2011), though one study reported that a more symmetrical arrangement was related to better phonological scores in girls (Yeatman et al., 2011). In the current study, higher FA and lower MD of the left arcuate, but not the right, were related to better language scores, consistent with previous research in children aged 3–10 (Cheema and Cummine, 2018), as well young children who have not yet begun reading (Saygin et al., 2013; Vandermosten et al., 2015; Walton et al., 2018). This finding warrants further research, as it could have implications for intervention approaches by highlighting grey matter regions to target for combined neurostimulation/behavioral reading interventions.

The positive relationships between left arcuate microstructure and pre-reading skills, in conjunction with an absence of relationships between asymmetry and pre-reading, suggests that asymmetry and any benefits it may confer for reading and language are still developing, and emerge after reading has begun. Alternatively, it is possible that language and reading abilities are primarily related to the structure and function of left hemisphere areas, and that previously-observed relationships with asymmetry are simply a by-product of faster development in left hemispheric regions.

Both brain structure and function in language regions continue to develop throughout childhood. Structurally, FA and white matter volume increase while MD decreases with age (Lebel et al., 2008; Reynolds et al., 2019; Yeatman et al., 2011). The arcuate fasciculus is one of the later developing white matter tracts, and shows protracted development into young adulthood (Giorgio et al., 2010; Lebel and Beaulieu, 2011). Functional connectivity also increases during childhood (Long et al., 2017; Xiao et al., 2016b). The patterns observed here are consistent with this prior developmental literature, and show that left hemisphere language regions develop slightly faster than right hemisphere regions. Given the relationships between the left arcuate microstructure and pre-reading, further research should be undertaken to explore how changes in pre-reading skills, intensive pre-reading instruction, and the extent of reading exposure at home may relate to arcuate development. All these factors could be important for informing reading intervention approaches for children at risk of developmental reading disorders.

There are some limitations of this study. Only linear age related trajectories were explored for arcuate microstructural, and structural and functional and asymmetry development. Further, only children over 2 years of age were included in this study; because asymmetry was found to be established by this age, future research is needed to identify whether asymmetry is established at birth, or during early infancy. Standard scores were used for all pre-reading assessments rather than raw scores, as a result of the changes in assessment measures over the age range of the study participants, and the large changes in raw pre-reading scores and tract-based measures with age during this period of development.

5. Conclusions

In conclusion, our large, longitudinal study shows that macrostructural asymmetry of the arcuate fasciculus is present by age 2 years, and that leftward asymmetry of microstructure and functional connectivity in language regions increases across early childhood, driven primarily by faster age-related changes in left hemisphere areas. An

absence of relationships between asymmetry and pre-reading skills suggests that this association may not be established until after children begin reading. Early childhood is a critical time of both language and brain development, and one in which the left-lateralized reading network is beginning to emerge. The substantial development of reading related tracts during this period of early childhood, and the relationships between brain structure and pre-reading skills prior to reading instruction, suggest that this age period is important for implementing early reading interventions.

Declaration of Competing Interest

The authors have no competing interests to declare.

Acknowledgements

The authors thank the members of the APrON study for assistance with recruitment.

Funding

This work was supported by the Canadian Institutes of Health Research (CIHR) (grant numbers IHD-134090, MOP-136797, New Investigator Award to C.L) and a grant from the Alberta Children's Hospital Foundation Awarded to D.D and C.L. J.E.R was supported by an Eyes High University of Calgary Postdoctoral Scholarship and a T. Chen Fong Fellowship in Medical Imaging Science. X.L was funded by the University of Calgary I3T program. M.N.G was supported by a University of Calgary Queen Elizabeth II Graduate Scholarship and a Vi Riddell Pediatric Rehabilitation Studentship.

Appendix A. Supplementary data

Supplementary material related to this article can be found, in the online version, at doi:https://doi.org/10.1016/j.dcn.2019.100682.

References

Bates, D., Mächler, M., Bolker, B., Walker, S., 2015. Fitting linear mixed-effects models using lme4. J. Stat. Softw. 67, 48. https://doi.org/10.18637/jss.v067.i01.

Bornstein, M.H., Hahn, C.-S., Haynes, O.M., 2004. Specific and general language performance across early childhood: stability and gender considerations. First Lang. 24, 267–304. https://doi.org/10.1177/0142723704045681.

Catani, M., Allin, M.P.G., Husain, M., Pugliese, L., Mesulam, M.M., Murray, R.M., Jones, D.K., 2007. Symmetries in human brain language pathways correlate with verbal recall. Proc. Natl. Acad. Sci. U. S. A. 104, 17163–17168. https://doi.org/10.1073/pnas.0702116104.

Cheema, K., Cummine, J., 2018. The relationship between white matter and reading acquisition, refinement and maintenance. Dev. Neurosci. 40, 209–222. https://doi.org/10.1159/000489491.

Cox, R.W., 1996. AFNI: software for analysis and visualization of functional magnetic resonance neuroimages. Comput. Biomed. Res. 29, 162–173. https://doi.org/10.1006/cbmr.1996.0014.

Dehaene-Lambertz, G., Dehaene, S., Hertz-Pannier, L., 2002. Functional neuroimaging of speech perception in infants. Science 298, 2013–2015. https://doi.org/10.1126/science.1077066.

Dehaene-Lambertz, G., Hertz-Pannier, L., Dubois, J., 2006a. Nature and nurture in language acquisition: anatomical and functional brain-imaging studies in infants. Trends Neurosci. 29, 367–373. https://doi.org/10.1016/j.tins.2006.05.011.

Dehaene-Lambertz, G., Hertz-Pannier, L., Dubois, J., Mériaux, S., Roche, A., Sigman, M., Dehaene, S., 2006b. Functional organization of perisylvian activation during presentation of sentences in preverbal infants. Proc. Natl. Acad. Sci. U. S. A. 103, 14240–14245. https://doi.org/10.1073/pnas.0606302103.

Dubois, J., Hertz-Pannier, L., Cachia, A., Mangin, J.F., Le Bihan, D., Dehaene-Lambertz, G., 2008. Structural asymmetries in the infant language and sensori-motor networks. Cereb. Cortex 19, 414–423. https://doi.org/10.1093/cercor/bhn097.

Eluvathingal, T.J., Hasan, K.M., Kramer, L., Fletcher, J.M., Ewing-Cobbs, L., 2007. Quantitative diffusion tensor tractography of association and projection fibers in normally developing children and adolescents. Cereb. Cortex 17, 2760–2768. https://doi.org/10.1093/cercor/bhm003.

Fonov, V., Evans, A.C., Botteron, K., Almli, C.R., McKinstry, R.C., Collins, D.L., Brain Development Cooperative Group, 2011. Unbiased average age-appropriate atlases for pediatric studies. NeuroImage 54, 313–327. https://doi.org/10.1016/j.neuroimage.2010.07.033.

Friederici, A.D., Brauer, J., Lohmann, G., 2011. Maturation of the language network: from inter-to intrahemispheric connectivities. PLoS One 6, e20726. https://doi.org/10.1371/journal.pone.0020726.

Giorgio, A., Watkins, K.E., Chadwick, M., James, S., Winmill, L., Douaud, G., De Stefano, N., Matthews, P.M., Smith, S.M., Johansen-Berg, H., 2010. Longitudinal changes in grey and white matter during adolescence. NeuroImage 49, 94–103 http://doi.org/j.neuroimage.2009.08.003.

Hickok, G., Poeppel, D., 2004. Dorsal and ventral streams: a framework for understanding aspects of the functional anatomy of language. Cognition 92, 67–99. https://doi.org/10.1016/j.cognition.2003.10.011.

Holland, S.K., et al., 2007. Functional MRI of language lateralization during development in children. Int. J. Audiol. 46, 533–551. https://doi.org/10.1080/14992020701448994.

Houdé, O., Rossi, S., Lubin, A., Joliot, M., 2010. Mapping numerical processing, reading, and executive functions in the developing brain: an fMRI meta-analysis of 52 studies including 842 children. Dev. Sci. 13, 876–885. https://doi.org/10.1111/j.1467-7687.2009.00938.x.

IBM Corp, 2016. IBM SPSS Statistics for Macintosh, Version 24.0. Released. IBM Corp., Armonk, NY.

Jenkinson, M., Bannister, P., Brady, M., Smith, S., 2002. Improved optimization for the robust and accurate linear registration and motion correction of brain images. NeuroImage 17, 825–841. https://doi.org/10.1006/nimg.2002.1132.

Jenkinson, M., Beckmann, C.F., Behrens, T.E., Woolrich, M.W., Smith, S.M., 2012. FSL. NeuroImage 62, 782–790. https://doi.org/10.1016/j.neuroimage.2011.09.015.

Kaplan, B.J., Giesbrecht, G.F., Leung, B.M.Y., Field, C.J., Dewey, D., Bell, R.C., Manca, D.P., O'Beirne, M., Johnston, D.W., Pop, V.J., 2014. The Alberta Pregnancy Outcomes and Nutrition (APrON) cohort study: rationale and methods. Matern. Child Nutr. 10, 44–60. https://doi.org/10.1111/j.1740-8709.2012.00433.x.

Korkman, M., Kirk, U., Kemp, S., 2007. NEPSY–Second Edition (NEPSY-II). The Psychological Corporation, San Antonio.

Kuznetsova, A., Brockhoff, P.B., Christensen, R.H.B., 2017. lmerTest package: tests in linear mixed effects models. J. Stat. Softw. 82, 26. https://doi.org/10.18637/jss.v082.i13.

Lebel, C., Beaulieu, C., 2009. Lateralization of the arcuate fasciculus from childhood to adulthood and its relation to cognitive abilities in children. Hum. Brain Mapp. 30, 3563–3573. https://doi.org/10.1002/hbm.20779.

Lebel, C., Beaulieu, C., 2011. Longitudinal development of human brain wiring continues from childhood into adulthood. J. Neurosci. 31, 10937–10947. https://doi.org/10.1523/JNEUROSCI.5302-10.2011.

Lebel, C., Treit, S., Beaulieu, C., 2017. A review of diffusion MRI of typical white matter development from early childhood to young adulthood. NMR Biomed. e3778. https://doi.org/10.1002/nbm.3778.

Lebel, C., Walker, L., Leemans, A., Phillips, L., Beaulieu, C., 2008. Microstructural maturation of the human brain from childhood to adulthood. NeuroImage 40, 1044–1055. https://doi.org/10.1016/j.neuroimage.2007.12.053.

Leemans, A., Jeurissen, B., Sijbers, J., Jones, D., 2009. ExploreDTI: a graphical toolbox for processing, analyzing, and visualizing diffusion MR data. Proc. Intl. Soc. Mag. Reson. Med. 17, 3537.

Leemans, A., Jones, D.K., 2009. The B-matrix must be rotated when correcting for subject motion in DTI data. Magn. Reson. Med. 61, 1336–1349. https://doi.org/10.1002/mrm.21890.

Logan, J.A., Schatschneider, C., Wagner, R.K., 2011. Rapid serial naming and reading ability: the role of lexical access. Read. Writ. 24, 1–25. https://doi.org/10.1007/s11145-009-9199-1.

Long, X., Benischek, A., Dewey, D., Lebel, C., 2017. Age-related functional brain changes in young children. NeuroImage 155, 322–330. https://doi.org/10.1016/j.neuroimage.2017.04.059.

Lonigan, C.J., Farver, J.M., Nakamoto, J., Eppe, S., 2013. Developmental trajectories of preschool early literacy skills: a comparison of language-minority and monolingual-English children. Dev. Psychol. 49, 1943–1957. https://doi.org/10.1037/a0031408.

May, L., Byers-Heinlein, K., Gervain, J., Werker, J.F., 2011. Language and the newborn brain: does prenatal language experience shape the neonate neural response to speech? Front. Psychol. 2, 222. https://doi.org/10.3389/fpsyg.2011.00222.

O'Muircheartaigh, J., Dean, D.C., Dirks, H., Waskiewicz, N., Lehman, K., Jerskey, B.A., Deoni, S.C.L., 2013. Interactions between white matter asymmetry and language during neurodevelopment. J. Neurosci. 33, 16170–16177. https://doi.org/10.1523/JNEUROSCI.1463-13.2013.

Pena, M., Maki, A., Kovačić, D., Dehaene-Lambertz, G., Koizumi, H., Bouquet, F., Mehler, J., 2003. Sounds and silence: an optical topography study of language recognition at birth. Proc. Natl. Acad. Sci. U. S. A. 100, 11702–11705. https://doi.org/10.1073/pnas.1934290100.

Perani, D., Saccuman, M.C., Scifo, P., Awander, A., Spada, D., Baldoli, C., Poloniato, A., Lohmann, G., Friederici, A.D., 2011. Neural language networks at birth. Proc. Natl. Acad. Sci. U. S. A. 108, 16056–16061. https://doi.org/10.1073/pnas.1102991108.

Pernet, C.R., Wilcox, R.R., Rousselet, G.A., 2013. Robust correlation analyses: false positive and power validation using a new open source Matlab toolbox. Front. Psychol. 3, 606. https://doi.org/10.3389/fpsyg.2012.00606.

Qiu, D., Tan, L.H., Siok, W.T., Zhou, K., Khong, P.L., 2011. Lateralization of the arcuate fasciculus and its differential correlation with reading ability between young learners and experienced readers: a diffusion tensor tractography study in a Chinese cohort. Hum. Brain Mapp. 32, 2054–2063. https://doi.org/10.1002/hbm.21168.

Raschle, N.M., Chang, M., Gaab, N., 2011. Structural brain alterations associated with dyslexia predate reading onset. NeuroImage 57 (3), 742–749.

Reynolds, J.E., Grohs, M.N., Dewey, D., Lebel, C., 2019. Global and regional white matter development in early childhood. NeuroImage 196, 49–58.

RStudio Team, 2016. RStudio: Integrated Development for R. URL. RStudio, Inc., Boston,

MA. http://www.rstudio.com.
Sakai, K.L., 2005. Language acquisition and brain development. Science 310, 815–819. https://doi.org/10.1126/science.1113530.
Salvan, P., Tournier, J.D., Batalle, D., Falconer, S., Chew, A., Kennea, N., Aljabar, P., Dehaene-Lambertz, G., Arichi, T., Edwards, A.D., 2017. Language ability in preterm children is associated with arcuate fasciculi microstructure at term. Hum. Brain Mapp. 38, 3836–3847. https://doi.org/10.1002/hbm.23632.
Satterthwaite, T.D., Elliott, M.A., Gerraty, R.T., Ruparel, K., Loughead, J., Calkins, M.E., Eickhoff, S.B., Hakonarson, H., Gur, R.C., Gur, R.E., 2013. An improved framework for confound regression and filtering for control of motion artifact in the preprocessing of resting-state functional connectivity data. NeuroImage 64, 240–256. https://doi.org/10.1016/j.neuroimage.2012.08.052.
Saur, D., Kreher, B.W., Schnell, S., Kümmerer, D., Kellmeyer, P., Vry, M.-S., Umarova, R., Musso, M., Glauche, V., Abel, S., 2008. Ventral and dorsal pathways for language. Proc. Natl. Acad. Sci. U. S. A. 105, 18035–18040. https://doi.org/10.1073/pnas.0805234105.
Saygin, Z.M., Norton, E.S., Osher, D.E., Beach, S.D., Cyr, A.B., Ozernov-Palchik, O., Yendiki, A., Fischl, B., Gaab, N., Gabrieli, J.D.E., 2013. Tracking the roots of reading ability: white matter volume and integrity correlate with phonological awareness in prereading and early-reading kindergarten children. J. Neurosci. 33, 13251–13258. https://doi.org/10.1523/JNEUROSCI.4383-12.2013.
Schlaggar, B.L., McCandliss, B.D., 2007. Development of neural systems for reading. Annu. Rev. Neurosci. 30, 475–503. https://doi.org/10.1146/annurev.neuro.28.061604.135645.
Smits, M., Jiskoot, L.C., Papma, J.M., 2014. White matter tracts of speech and language. Semin. Ultrasound CT MR 35, 504–516. https://doi.org/10.1053/j.sult.2014.06.008.
Song, J.W., Mitchell, P.D., Kolasinski, J., Ellen Grant, P., Galaburda, A.M., Takahashi, E., 2014. Asymmetry of white matter pathways in developing human brains. Cereb. Cortex 25, 2883–2893. https://doi.org/10.1093/cercor/bhu084.
Szaflarski, J.P., Holland, S.K., Schmithorst, V.J., Byars, A.W., 2006. fMRI study of language lateralization in children and adults. Hum. Brain Mapp. 27, 202–212. https://doi.org/10.1002/hbm.20177.
Tak, H.J., Kim, J.H., Son, S.M., 2016. Developmental process of the arcuate fasciculus from infancy to adolescence: a diffusion tensor imaging study. Neural Regen. Res. 11, 937–943. https://doi.org/10.4103/1673-5374.184492.
Thieba, C., Frayne, A., Walton, M., Mah, A., Benischek, A., Dewey, D., Lebel, C., 2018. Factors associated with successful MRI scanning in unsedated young children. Front. Pediatr. 6, 146. https://doi.org/10.3389/fped.2018.00146.
Torppa, M., Poikkeus, A.-M., Laakso, M.-L., Eklund, K., Lyytinen, H., 2006. Predicting delayed letter knowledge development and its relation to grade 1 reading achievement among children with and without familial risk for dyslexia. Dev. Psychol. 42, 1128–1142. https://doi.org/10.1037/0012-1649.42.6.1128.
Vandermosten, M., Boets, B., Poelmans, H., Sunaert, S., Wouters, J., Ghesquiere, P., 2012. A tractography study in dyslexia: neuroanatomic correlates of orthographic, phonological and speech processing. Brain 135, 935–948. https://doi.org/10.1093/brain/awr363.
Vandermosten, M., Vanderauwera, J., Theys, C., De Vos, A., Vanvooren, S., Sunaert, S., Wouters, J., Ghesquière, P., 2015. A DTI tractography study in pre-readers at risk for dyslexia. Dev. Cogn. Neurosci. 14, 8–15. https://doi.org/10.1016/j.dcn.2015.05.006.
Vigneau, M., Beaucousin, V., Herve, P.-Y., Duffau, H., Crivello, F., Houde, O., Mazoyer, B., Tzourio-Mazoyer, N., 2006. Meta-analyzing left hemisphere language areas: phonology, semantics, and sentence processing. NeuroImage 30, 1414–1432. https://doi.org/10.1016/j.neuroimage.2005.11.002.
Wakana, S., Jiang, H., Nagae-Poetscher, L.M., Van Zijl, P.C., Mori, S., 2004. Fiber tract–based atlas of human white matter anatomy. Radiology 230, 77–87. https://doi.org/10.1148/radiol.2301021640.
Walton, M., Dewey, D., Lebel, C., 2018. Brain white matter structure and language ability in preschool-aged children. Brain Lang. 176, 19–25. https://doi.org/10.1016/j.bandl.2017.10.008.
Xia, M., Wang, J., He, Y., 2013. BrainNet Viewer: a network visualization tool for human brain connectomics. PLoS One 8, e68910. https://doi.org/10.1371/journal.pone.0068910.
Xiao, Y., Brauer, J., Lauckner, M., Zhai, H., Jia, F., Margulies, D.S., Friederici, A.D., 2016a. Development of the intrinsic language network in preschool children from ages 3 to 5 years. PLoS One 11, e0165802. https://doi.org/10.1371/journal.pone.0165802.
Xiao, Y., Zhai, H., Friederici, A.D., Jia, F., 2016b. The development of the intrinsic functional connectivity of default network subsystems from age 3 to 5. Brain Imaging Behav. 10, 50–59. https://doi.org/10.1007/s11682-015-9362-z.
Yamada, Y., Stevens, C., Dow, M., Harn, B.A., Chard, D.J., Neville, H.J., 2011. Emergence of the neural network for reading in five-year-old beginning readers of different levels of pre-literacy abilities: an fMRI study. NeuroImage 57, 704–713. https://doi.org/10.1016/j.neuroimage.2010.10.057.
Yeatman, J.D., Dougherty, R.F., Rykhlevskaia, E., Sherbondy, A.J., Deutsch, G.K., Wandell, B.A., Ben-Shachar, M., 2011. Anatomical properties of the arcuate fasciculus predict phonological and reading skills in children. J. Cogn. Neurosci. 23, 3304–3317. https://doi.org/10.1162/jocn_a_00061.
Youssofzadeh, V., Vannest, J., Kadis, D.S., 2018. fMRI connectivity of expressive language in young children and adolescents. Hum. Brain Mapp. https://doi.org/10.1002/hbm.24196. Online ahead of print.